Journal of Inflammation Research Dovepress

Open Access Full Text Article ORIGINAL RESEARCH

Alterations of Hepatic Lipidome Occur in a Gouty Model: A Shotgun Lipidomics Study

Xiaofen Xu[1,*], Wumeng Jin[1,*], Jingyi Song[1], Xuanming Hu[1], Lu Lu[2], Jida Zhang[1], Changfeng Hu[1]

[1]College of Basic Medical Sciences, Zhejiang Chinese Medical University, Hangzhou, Zhejiang, 310053, People's Republic of China; [2]Third Clinical Medical College, Zhejiang Chinese Medical University, Hangzhou, Zhejiang, 310005, People's Republic of China

*These authors contributed equally to this work

Correspondence: Jida Zhang; Changfeng Hu, College of Basic Medical Sciences, Zhejiang Chinese Medical University, Hangzhou, Zhejiang, People's Republic of China, Email zhjd82@tom.com; zhudianzhuifeng@163.com

Background: Liver injury, such as nonalcoholic fatty liver disease, is a common symptom observed in patients with gout/hyperuricaemia. However, the exact mechanisms are still unclear. There is ongoing controversy about whether representative agents like colchicine and febuxostat, commonly used to manage gout, could also help prevent the liver injury. Liver plays a crucial role in uric acid (UA) production and lipid metabolism. Thus, the study aimed to investigate the aberrant lipid metabolism in the liver during injury and the effects of these drugs.

Methods: An advanced multi-dimensional mass spectrometry-based shotgun lipidomics technology was employed for class-targeted lipid analysis of cellular lipidomes in hepatic tissue of a gouty model induced by a combination of monosodium urate crystals and high-fat diet with or without treatment with colchicine and febuxostat. Serum UA, blood urea nitrogen, creatinine, proinflammatory cytokines, expression of AMP-activated protein kinase protein, footpad histopathology, and footpad swelling and pain threshold of these mice were assessed to evaluate the progression of gout.

Results: Lipidomics analysis clearly demonstrated that the ectopic fat accumulation as well as changes in fatty acyls composition in TAG pool, impaired mitochondrial function resulted by decreased tetra 18:2 cardiolipin, and reduced 4-hydroxyalkenal bioavailability in liver tissue could contribute to liver damage to the gouty model. Treatment with colchicine or febuxostat not only ameliorated gouty symptoms but also corrected these abnormal hepatic lipid metabolism patterns.

Conclusion: This study shed light on underlying mechanism(s) for liver injury in gout/hyperuricaemia and suggested that administration of drugs like colchicine and febuxostat could prevent liver injury.

Keywords: gout, hepatic lipidome, febuxostat, colchicine, inflammation

Introduction

Gout, a chronic and inflammatory disease, is caused by the deposition of monosodium urate (MSU) crystals in both articular and non-articular structures.[1] The hallmark symptoms of gout encompass intense pain, swelling, warmth, fever, redness, and tenderness at the gouty joint. Elevated serum uric acid (UA) level stands out as the foremost risk factor for gout development, with a serum UA level of ≥0.42 mmol/L indicative of hyperuricaemia (exceeding the saturation threshold), which could trigger the deposition of MSU crystals, and consequently, gout. Presently, gout stands as the most prevalent form of inflammatory arthritis.[2] Furthermore, population-based studies across Asia, Europe, and North America indicate a steady rise in the prevalence and incidence of gout/hyperuricaemia.[3] In clinical practice, the primary approach to effectively managing gout involves urate-lowering treatment, aimed at reducing serum UA either through the inhibition of xanthine oxidase (XOD, a rate-limiting enzyme in UA production) or by increasing the renal excretion of UA. Therefore, colchicine, nonsteroidal anti-inflammatory drugs, and urate-lowering medicines (such as febuxostat) are the representative agents employed in the treatment of gout.[4]

Received: 13 August 2024
Accepted: 24 October 2024
Published: 29 October 2024

Liver injury, such as non-alcoholic fatty liver disease (NAFLD), is one of the most prevalent manifestations of patients with gout/hyperuricaemia. Numerous studies have underscored the strong correlation between NAFLD and gout/hyperuricaemia.[5,6] Liver serves as the primary tissue for production of UA, predominantly derived from purine nucleotides through the action of XOD. While several studies have highlighted the link between elevated serum UA level and NAFLD, indicating hyperuricaemia as a potentially significant independent contributor to NAFLD development, the precise underlying mechanism(s) remain elusive.[7] NAFLD is characterized by excessive accumulation of lipids in blood and hepatocytes. Despite the observed elevation in cholesterol and triglycerides (TAGs) levels in both liver and circulation in NAFLD, comprehensive studies on hepatic lipid metabolism in gout-related models are scarce. Lipids and their metabolites, beyond their role as fundamental components of cell membranes, play pivotal roles in diverse biological processes such as energy storage, signaling transduction, and cellular growth, differentiation and survival.[8] Furthermore, dysregulated lipid metabolism has been linked to the activation of immune responses and inflammatory reactions, including the stimulation of autoantibody production and inflammatory cytokines, thereby drastically accelerating the progression of associated diseases.[9,10]

Additionally, the potential of anti-inflammatory drugs and urate-lowering medicines to prevent liver injury of patients with gout/hyperuricaemia remains a topic of debate. For instance, it has been reported that colchicine, a systemic anti-inflammatory agent commonly employed in gout management, might trigger hepatotoxicity, potentially exacerbating the development of NAFLD.[11] Furthermore, the impact of febuxostat administration on liver injury through modulation of hepatic lipid metabolism remains uncertain.[12] Therefore, investigating alterations in hepatic lipid profiles could greatly facilitate understanding of the underlying mechanism(s) contributing to liver injury in patients with gout/hyperuricaemia, as well as help evaluate the effects of various therapeutic approaches.

As kidney injury is one of the most common clinical manifestations in patients with hyperuricemia/gout, and lipids play a crucial role in almost all vital biological processes, especially in maintaining kidney function, our previous research focused on the induced gout model via a combination of urate crystal injection and high-fat diet. In the earlier study, we performed targeted lipidomic analysis on the kidney tissues to identify the primary factors contributing to kidney damage in gout, discovering significant lipid metabolism abnormalities in the kidneys of these model mice, including alterations in TAG and HNE.[13] It is well known that the liver is the primary site for the production of uric acid as well as a major organ for lipid metabolism. Based on the previous findings of significant lipid metabolism disorders in the renal tissues of the gout model, this study further investigated the expression of related lipids in the liver tissues of the model mice to clarify the crucial role of lipid metabolism disorders in the pathogenesis of high-fat and high-uric acid conditions.

In the study, an advanced multi-dimensional mass spectrometry-based shotgun lipidomics (MDMS-SL) technology was utilized to conduct a comprehensive analysis of cellular lipidomes in hepatic tissue from a gouty model induced by a combination of MSU crystal injection and a high-fat diet (HFD), with or without treatment using medications such as colchicine and febuxostat. The analyzed lipids included TAGs as well as the composition of various fatty acyls (FAs) in TAG pool, 4-hydroxyalkenal species, various classes of phospholipids (eg, cardiolipin (CL), choline glycerophospholipid (PC), ethanolamine glycerophospholipid (PE), phosphatidic acid (PA), phosphatidylserine (PS), phosphatidylinositol (PI), and phosphatidylglycerol (PG)) and relevant lysophospholipids (such as choline lysoglycerophospholipid (LPC) and ethanolamine lysoglycerophospholipid (LPE)), sphingolipids (ie, ceramide and sphingomyelin (SM)) species, etc. Additionally, determination of serum UA, blood urea nitrogen (BUN), creatinine, proinflammatory cytokines, and AMPK protein expression, footpad histopathology, and footpad swelling and pain threshold in mice from each group to evaluate the onset and outcomes of gout, revealing the mechanisms underlying liver injury and the effects of different therapeutic interventions.

Materials and Methods

Materials

All synthetic phospholipids or other lipids, such as triheptadecenoyl glycerol (T17:1 TAG), 1.2-dimyristoleoyl-*sn*-glycero-3-phosphocholine (di14:1 PC), 1-heptadecanoyl-2-hydroxy-*sn*-glycero-3-phosphocholine (17:0 LPC), 1.2-dipalmitoleoyl-*sn*-glycero-3-phosphoethanolamine (di16:1 PE), 1-myristoyl-2-hydroxy-*sn*-glycero-3-phosphocholine (14:0 LPE), 1',3'-bis [1,2-dimyristoyl-*sn*-glycero-3-phospho]-glycerol (ammonium salt) (tetra 14:0 CL), 1.2-dimyristoyl-*sn*-glycero-3-phospho-

L-serine (sodium salt) (di14:0 PS), 1.2-dimyristoyl-*sn*-glycero-3-phosphate (sodium salt) (di14:0 PA), and 4-hydroxy-*9,9,9-d3*-2 (*E*)-nonenal (4-HNE-*d3*) (100 μg in 200 μL of methyl acetate), used as internal standards were purchased from Avanti Polar Lipid, Inc. (Alabaster, AL, USA), Cayman Chemical Co. (Ann Arbor, MI, USA), or Matreya, Inc. (Pleasant Gap, PA, USA). All the solvents and chemicals were at least the analytical grade and brought from Merck KGaA (Darmstadt, Germany), Sigma-Aldrich Chemical Company (St. Louis, MO, USA), or Fisher Scientific (Pittsburgh, PA, USA).

Animal Experiments

Forty specific pathogen-free (SPF) male C57BL/6 mice (6 weeks old) bought from Shanghai SLAC Laboratory Animal Co., Ltd. were maintained in the SPF environment of the Center Animal House of Zhejiang Chinese Medical University. The animal experiments conducted in this study adhered to the guidelines established by the National Institutes of Health (NIH) for the Care and Use of Laboratory Animals. All animal experiments were approved by the Ethics Committee of Zhejiang Chinese Medical University with the approved No. IACUC-20220913-16. All information reported here was elaborated according to the ARRIVE guidelines. The mice were kept in cages under a 12:12 h light and dark cycle and an ambient temperature (22–25 °C) and humidity (50 ± 5%) with free access to food and water.

After 7 days of acclimatization, the mice were randomly divided into four groups (10 mice per group), including control, gouty model, gouty model-colchicine treatment (the colchicine), and gouty model-febuxostat treatment (the febuxostat) groups. The mice in the control group were fed with a normal diet and injected with 40 μL of PBS in the right hind footpad every 7 days. The mice in the other three groups were fed with a high-fat diet (10% yeast extract) and injected with MSU crystals (1 mg MSU crystals in 40 μL of PBS) every 7 days to establish the gouty model.[14] In addition, the colchicine and the febuxostat groups were treated with colchicine (0.78 mg/Kg/week) and febuxostat (5.2 mg/Kg/day), respectively.[15] Incidentally, after the mice were injected with MSU crystals, the colchicine group was administrated with colchicine immediately, while the febuxostat group was fed with febuxostat after 12 h to avoid the acute phase as much as possible. The mice in control and model groups were orally fed with the same volume of distilled water.

After being treated for 6 weeks, all of the mice were euthanized with CO_2, and samples were collected at 12 h after the last administration and injection of MSU. Blood was collected by retro-orbital puncture and further centrifuged (1300 *g*, 15 min, 4 °C) to get serum samples. Hepatic tissues were also collected, lavaged with PBS to remove blood, and then stored at −80 °C for lipid analysis. Meanwhile, foot joint tissue samples were also collected and stored at −80 °C.

Assessment of Gouty Onset and/or Outcome

Determination of Serum UA and Proinflammatory Cytokines

200 μL of serum for each sample of mice from different groups was used for determining levels of serum UA and BUN. Their concentrations were measured by automatic biochemical analyzer (TOSHIBA TBA-120FR, Toshiba Medical Systems Co., Tochigi, Japan) following the manufacturer's operation instructions. Proinflammatory cytokines, including IL-1β, IL-6, and TNF-α, in serum samples of each mouse were determined by mouse ELISA Commercial Kits (Jianglai Biotechnology Co., Ltd., Shanghai, China). Their levels were calculated depending on the standard curves.

Moreover, XOD and adenosine deaminase (ADA) activities in hepatic tissue were also determined. Briefly, each liver sample was pulverized into fine powder with a stainless-steel mortar and pestle under the temperature of liquid nitrogen. The powder samples were further homogenized (50 mg per 1.0 mL buffer solution for each) and centrifuged (12,000 rpm, 10 min, 4 °C) to isolate the supernatant. Then, these obtained supernatant samples were subjected to determine XOD and ADA activities according to the manufacturer's instructions (Jiangcheng, Nanjing, China).

Evaluation of Footpad Swelling and Pain Threshold

As previously reported, the footpad thickness of each mouse was determined with a caliper (Meinaite, Germany) before and at 4, 24, 48, and 72 h after injected MSU crystals into the footpads.[16] The ratio of Δmm/mm (at zero time point) of the joint was used to reflect the extent of foot swelling. In addition, the mechanical retreat threshold was measured by Von Frey filaments (Stoelting, Wood Dale, IL) to evaluate the foot pain threshold of mice according to the previous report.[17]

Histopathological Evaluation

Histopathological evaluation of the footpad was performed as previously described.[18,19] Briefly, each mouse tissue was fixed in 4% paraformaldehyde and subjected to routine paraffin embedding. After cut at a thickness of 4–6 μm, serial sections were stained with hematoxylin and eosin (H&E) and a modified Masson's trichrome kit. A Leica microscope equipped with a color CCD camera was used to acquire all the images.

Western Blot Analysis

Protein lysates were prepared from hepatic tissue employing RIPA lysis buffer supplemented with 1 mm PMSF (a protease inhibitor) as previously described.[14] Specifically, the protein concentration was measured by BCA protein assay (Pierce, Thermo Fisher Scientific Inc., San J ose, CA, USA). 40 μg of total protein was loaded per lane for SDS-PAGE (10% w/v) analysis and then transferred to a nitrocellulose membrane. After blocked with 5% BSA in TBST (Tri-buffered saline with 0.1% Tween-20), the membranes were incubated with primary antibodies. Then the membranes were washed with TBST and incubated using a secondary antibody. Proteins were visualized and validated with an infrared imaging system (Odyssey CLx; Li-COR Biosciences, Lincoln, NE, USA) and ImageJ software. The original gel and blot image are available in Figure S1 for reference.

Preparation of Lipid Extracts from Hepatic Samples

According to the previous report,[20] the lipids of individual liver sample (~25mg) were extracted by using a modified protocol of Bligh and Dyer in the presence of internal standards.[19] Each lipid extract was redissolved with 200 μL $CHCl_3$ /MeOH (1:1, *v/v*)/mg protein and then stored at −20 °C for lipid analysis. Derivatization of HNE species with carnosine and the primary amine in phosphoethanolamine-containing species (eg, PE and lysoPE) with fluorenylmethoxycarbonyl chloride was conducted as previously described, respectively.[21–23] Individual lipid species including FA isomers and regioisomers were identified using multi-dimensional MS analysis.[24,25] Incidentally, lipid analysis was finished within one week after the lipid extracts were prepared.

Lipid Analysis, and Data Processing and Analysis

Lipidomic analysis of liver samples was conducted with a triple-quadrupole mass spectrometer (Thermo TSQ Quantiva, Thermo Fisher Scientific Inc., San Jose, CA, USA) equipped with an automated nanospray ion source (TriVersa NanoMate, Advion Bioscience Ltd., Ithaca, NY, USA) according to the previous report.[26] To avoid possible lipid aggregation, the solutions of lipid extracts were further diluted in $CHCl_3$/MeOH/isopropyl alcohol (1:2:4, *v/v/v*) before being subjected to mass spectrometer. All mass spectral data were acquired by different customized sequence subroutines operated under Xcalibur software. Data processing was performed according to the previous report.[24] All data were presented at mean ± SEM unless otherwise indicated. Statistical significance among the groups (n=5) was performed by using ANOVA followed by Dunn multiple comparison with IBM SPSS Statistics 19 Software (SPSS Inc., Chicago, IL, USA), where $*p < 0.05$, $**p < 0.01$, and $***p < 0.001$.

Results

The Severity of Gouty Onset in Mice from Different Groups

To assess the development of a gouty model induced by the combination of MSU crystal injection and a high-fat diet, as well as the efficacy of different treatments, representative symptoms such as footpad swelling, pain threshold, and serum UA levels were evaluated in mice. The model mice exhibited a significant increase in serum UA levels, marked foot joint swelling, and a decrease in footpad mechanical pain threshold following MSU injection compared to control mice (Figure 1). Meanwhile, compared with the model group, along with the concentration of serum UA recovered to normal level, these indicators could also be evidently alleviated after treatment with either colchicine or febuxostat (Figure 1). Thus, as expected, both of these two therapies could effectively relieve the gouty symptoms to some extent.

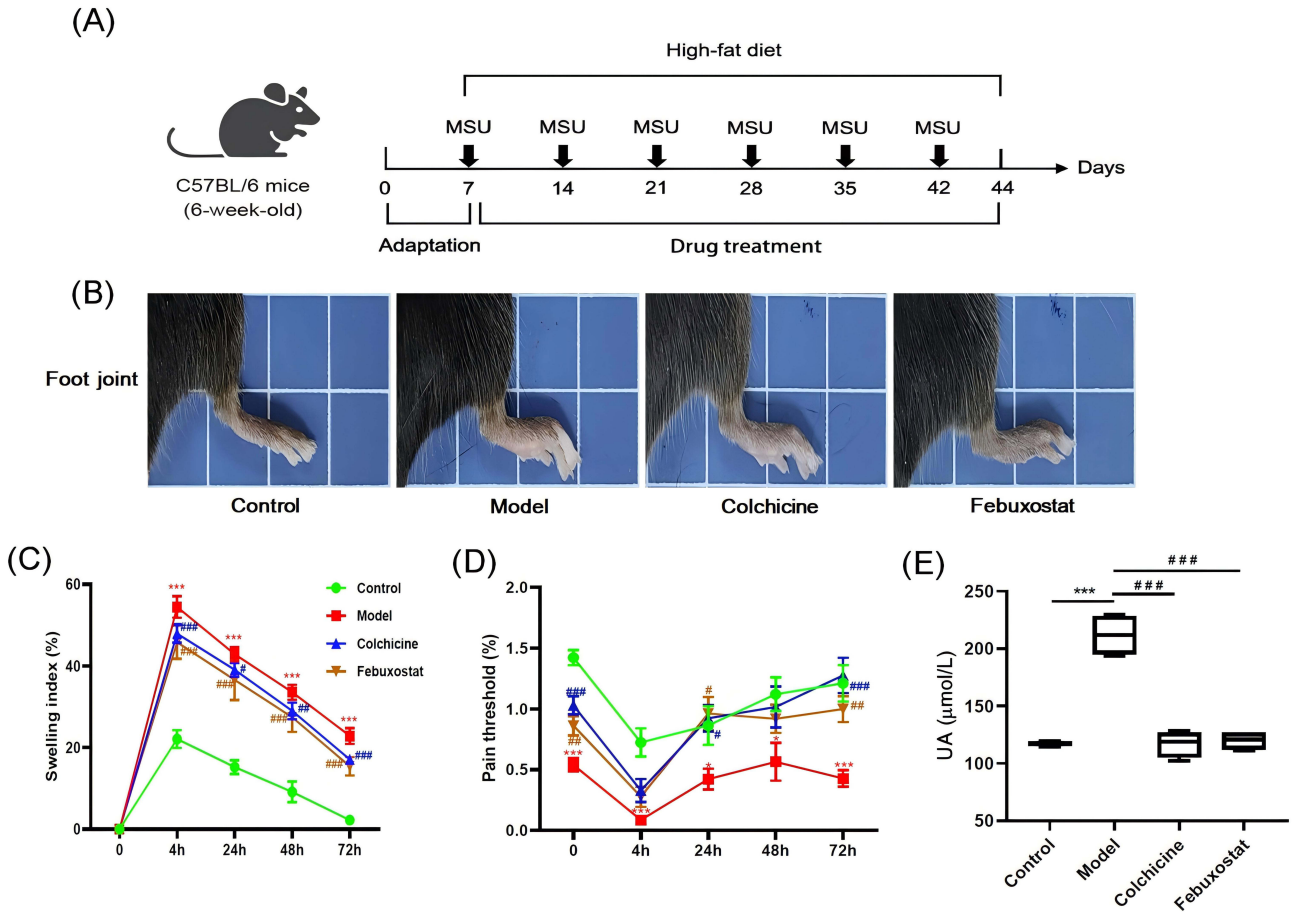

Figure 1 The gouty onset and severity, and/or outcome of mice from different groups. The diagram of the experimental treatments (**A**). Representative images of foot joints (**B**), footpad swelling index (**C**), footpad pain threshold (**D**), and serum UA (**E**) of mice from the control, model, colchicine, and febuxostat groups (n= 8/group). The data present means ± SEM from different groups. $^{*}p < 0.05$ and $^{***}p < 0.001$ compared with those in the control group. $^{\#}p < 0.05$, $^{\#\#}p < 0.01$, and $^{\#\#\#}p < 0.001$ compared with those in the model group. UA stands for uric acid.

Histopathological Evaluation and Inflammatory Responses of Mice from Different Groups

Given that inflammation is one of the hallmark symptoms of gout, histopathological evaluation of footpad was conducted to assess the extent of inflammation at gouty sites in mice from different groups.[13] As shown in the images of H&E staining analysis of the footpad, the model mice exhibited marked inflammatory cell infiltration and synovial hyperplasia in the foot joints. However, following treatment with either colchicine or febuxostat, the number of inflammatory cells in the foot joints was substantially reduced, indicating that both compounds were able to effectively inhibit the inflammatory responses in the footpad (Figure 2A).

As previously reported, the levels of certain proinflammatory cytokines, such as TNF-α, IL-1β, and IL-6, were found to be significantly elevated in patients with gout, suggesting heightened inflammatory responses in the gouty patient population.[27] Accordingly, the expression levels of these three proinflammatory cytokines in serum samples from different groups were determined using corresponding ELISA kits. The results clearly indicated that, compared with these of the control mice, the levels of all three cytokines in serum were substantially increased in the gouty mice (Figure 2B–D). Meanwhile, following treatment with colchicine or febuxostat, the levels of these proinflammatory mediators were reduced to some degree (Figure 2B–C), further supporting the notion that both of these therapeutic interventions were able to effectively attenuate the inflammatory responses in the gouty mice.

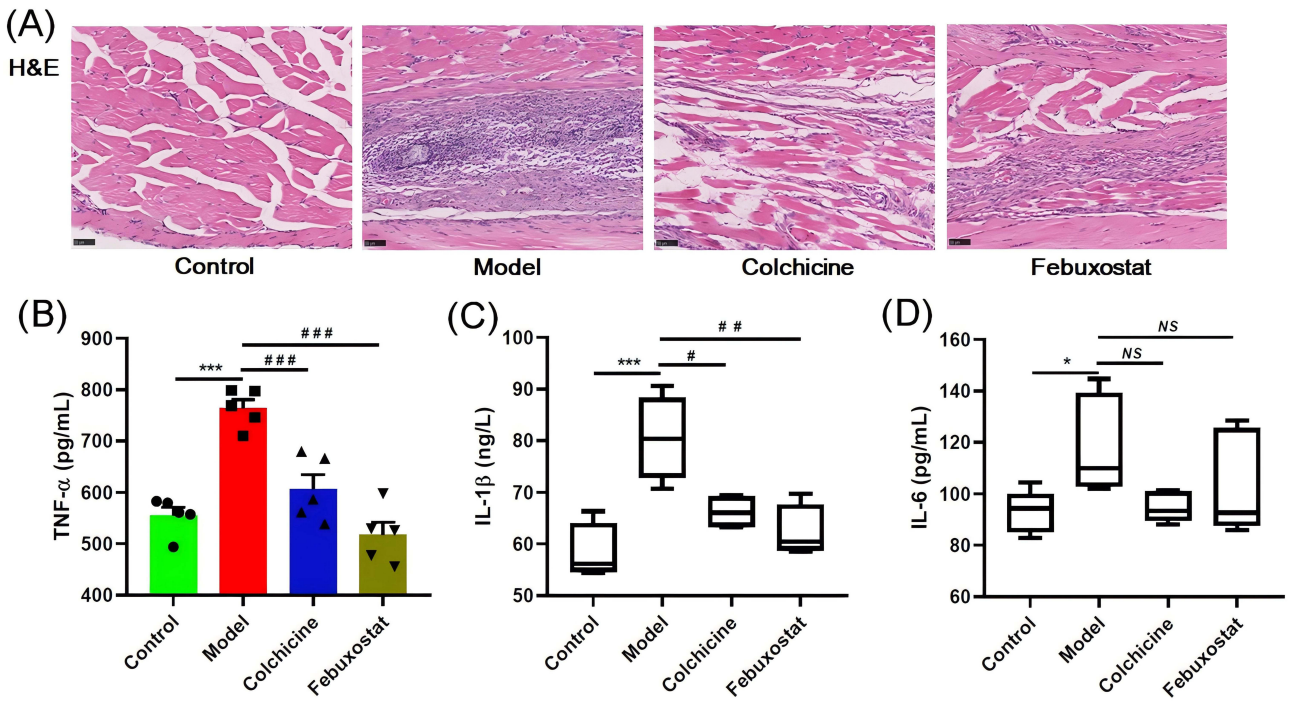

Figure 2 Inflammatory responses of the gouty mice from different groups. Representative images of hematoxylin and eosin (H&E) staining analysis of the footpad of mice from different groups (n= 8/group) (**A**). The levels of TNF-α (**B**), IL-1β (**C**), and IL-6 (**D**) in serum samples of mice from the four groups (n= 5/group) were measured with corresponding ELISA kits. The data present means ± SEM from different groups. $^{*}p < 0.05$ and $^{***}p < 0.001$ compared with those in the control group. $^{\#}p < 0.05$, $^{\#\#}p < 0.01$, and $^{\#\#\#}p < 0.001$ compared with those in the model group. *NS* denotes not significant.

Purine Metabolism in Hepatic Tissue and Renal Function of Mice from Different Groups

To evaluate the content of purine metabolism, ADA and XOD activities in hepatic tissues of mice from the four groups were also determined with corresponding ELISA kits. Specifically, as shown in Figure 3A, the ADA activity in the model group was not significantly altered compared with that of the control group. Treatment with either colchicine or febuxostat could reduce the ADA activity to some degree, although there was no remarkable difference in comparison with that of the model group. Additionally, the XOD activity in the model mice was markedly elevated in comparison with that of the control mice ($p < 0.01$). Furthermore, treatment with colchicine could effectively reduce its activity ($p < 0.01$, Figure 3B). Therefore, these results indicated that administration of either colchicine or febuxostat decreased UA by inhibiting activities of these two enzymes to some extent. Furthermore, the elevated level of blood urea nitrogen in mice from the model group indicated that kidney function of the gouty mice was impaired. Incidentally, significantly reduced levels of BUN and creatinine in the two treated groups also suggested that treatment with either colchicine or febuxostat could alleviate the renal injury of the gouty mice (Figure 3C and D).

Lipidomics Revealed Fat Accumulation in Hepatic Tissue of Gouty Mice

It is well known that ectopic fat deposition in hepatocytes greatly impairs the function of liver tissue, promoting the development of NAFLD as well as other hepatic diseases. Thus, the levels of TAG species as well as the composition of FA species in TAG pool were determined by using the MDMS-SL technology. The results of lipidomics analysis clearly suggested that the total amount of TAGs in hepatic tissue of mice from the model group was significantly elevated, resulting in an increase from 157.49 ± 10.13 in the control to 229.39 ± 13.59 nmol/mg protein in the model (an ~46 mol% elevation, $p < 0.001$) (Figure 4A). Moreover, the composition of FAs in TAG pool in mice from the model group was also substantially altered in comparison with that of the control. The alteration could be mainly attributed to the changes of two predominant FA species (ie, 18:1 and 18:2 FA species). Specifically, in comparison with these of the control, the composition of 18:1 FA in TAG pool of hepatic tissue from the model mice drastically increased (eg, 22.45 ± 0.79 and 42.57 ± 2.24 mol% in the control and the

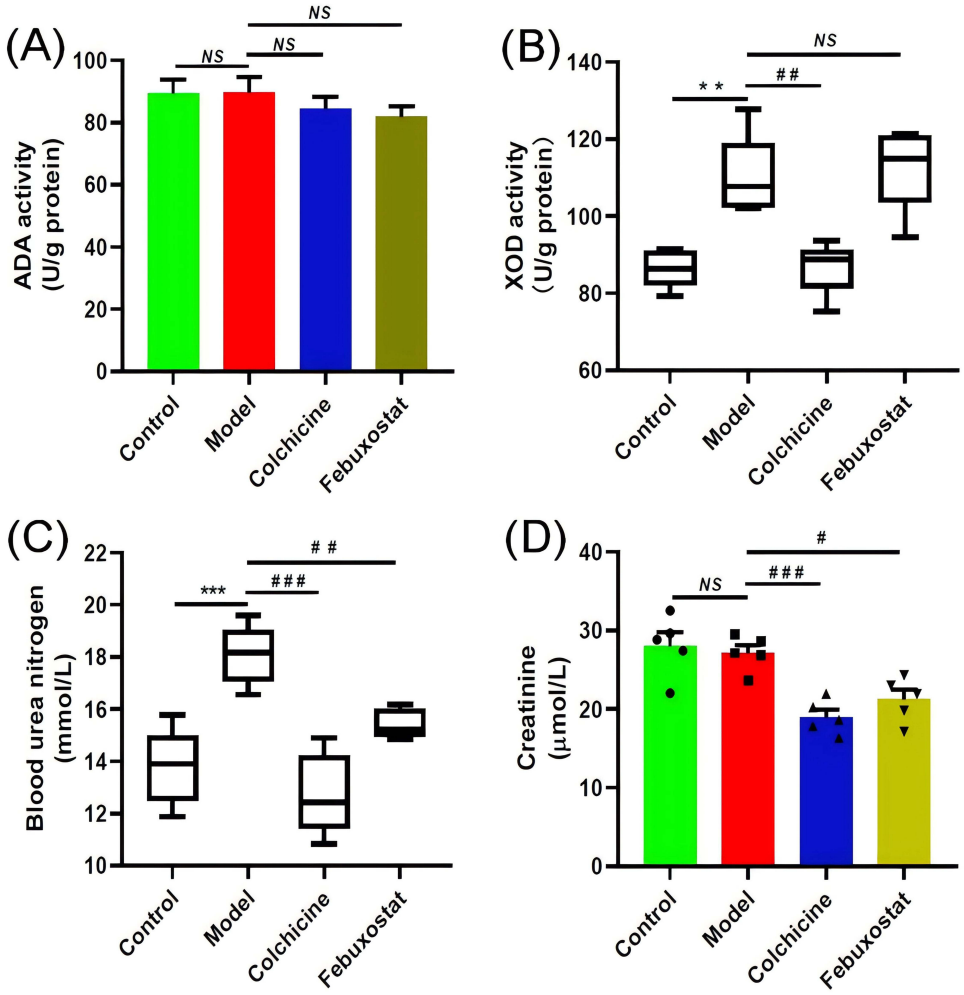

Figure 3 Purine metabolism in hepatic tissue and renal function of gouty mice from different groups. Levels of adenosine deaminase (**A**) and xanthine oxidase (**B**) activity related to purine metabolism in mouse hepatic tissue from the control, model, colchicine, and febuxostat groups (n= 5/group) were determined with ELISA kits. Levels of blood urea nitrogen (**C**) and creatinine (**D**) were measured to reflect the kidney function of mice from the four groups. The data present means ± SEM from different groups. $^{**}p < 0.01$ and $^{***}p < 0.001$ compared with those in the control group. $^{\#}p < 0.05$, $^{\#\#}p < 0.01$, and $^{\#\#\#}p < 0.001$ compared with those in the model group. *NS* means not significant. ADA and XOD stand for adenosine deaminase and xanthine oxidase, respectively.

model, respectively, $p < 0.001$), whereas the composition of 18:2 FA markedly decreased from 28.76 ± 0.94 in the control to 14.59 ± 0.38 mol% in the model ($p < 0.001$, Figure 4B). These results indicated that not only the accumulation of fat but also the altered composition of FAs in TAG pool was present in hepatic tissue of mice from the gouty model. Intriguingly, treatment with either colchicine or febuxostat could greatly prevent the fat deposition in liver tissue, nearly restoring to the normal level, that is, compared with that of the model group, the total amount of TAG markedly reduced to 155.17 ± 5.67 and 129.98 ± 3.38 nmol/mg protein in colchicine and febuxostat groups, respectively ($p < 0.001$). Incidentally, the changed composition of FA species in TAG pool could not be completely corrected by administration of either colchicine or febuxostat (Figure 4B).

Lipidomics Demonstrated the Aberrant Metabolism of Mitochondrial Function-Related Lipids in Hepatic Tissue of Gouty Mice

According to the previous report, high UA could induce mitochondrial dysfunction, thereby leading to hepatic steatosis.[28] CL is one class of atypical phospholipid composed by four fatty acyl chains and located mainly in the inner mitochondrial membrane. CL, especially tetra 18:2 CL, serves a crucial role in optimal mitochondrial function, such as optimal activities of respiratory chain complexes and ADP-ATP translocase involved in production of ATP and reactive oxygen species (ROS).[29] Therefore, the content of tetra 18:2 CL is an important index of mitochondrion, directly

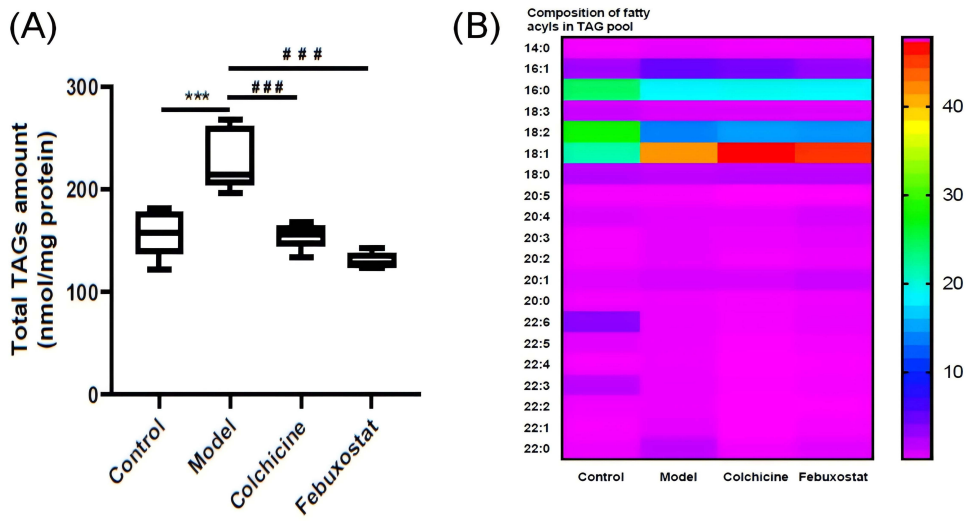

Figure 4 Lipidomics revealed fat deposition in hepatic tissue of gouty mice. Total amount of TAG species (**A**) and composition of fatty aclys species in TAG pool (**B**) in mouse hepatic tissue from the control, model, colchicine, and febuxostat groups (n= 5/group) were determined by the multidimensional mass-spectrometry-based shotgun lipidomics technology. The data present means ± SEM from different groups. ***p < 0.001 and $^{\#\#\#}p$ <0.001 compared with that of the control and the model group, respectively.

influencing production of ATP. As aforementioned, not only fat deposition but also significantly reduced composition of 18:2 FA in TAG pool was present in hepatic tissue of the gouty mice. Therefore, there was one question about whether the similar alteration in composition of 18:2 FA in TAG pool also exists in CL species, resulting in a low level of tetra 18:2 CL. In other words, the question is whether the mitochondrial dysfunction of hepatic tissue in the gouty model was impaired by reduced tetra 18:2 CL or not. To test the hypothesis, the MDMS-SL technology was performed to determine the level of CL species in hepatic tissues of mice from different groups. The result of lipidomics analysis clearly demonstrated that, the level of tetra 18:2 CL in hepatic tissue from the gouty mice significantly decreased in comparison with that of the control group ($p < 0.001$, Figure 5A). Moreover, after treatment with either colchicine or febuxostat, tetra 18:2 CL was markedly elevated ($p < 0.05$, Figure 5A). It indicated that either colchicine or febuxostat might recover mitochondrial dysfunction of hepatic tissue in gouty mice by increasing the content of tetra18:2 CL.

Since the primary function of mitochondrion is to yield large quantities of ATP, the impaired mitochondrial function inevitably results in low energy supply. Under falling cellular energy status, the metabolic sensor AMP-activated protein kinase (AMPK) would be activated to regulate cellular energy balance.[30] Thus, to further confirm mitochondrial dysfunction in hepatic tissue of the gouty mice led by reduced levels of tetra 18:2 CL, the expression of AMPK protein in liver samples from different groups was assessed by Western blot analysis. The expression of AMPK in hepatic tissue from the model mice was significantly elevated accompanying with the remarkable low level of tetra 18:2 CL (Figure 5B). The result further demonstrated that the reduced production of ATP was present in hepatic tissue from the gouty model. Moreover, along with the increased levels of tetra 18:2 CL in the colchicine and febuxostat groups, the expression of AMPK markedly decreased in comparison with that of the model group, further demonstrating that treatment with either colchicine or febuxostat could improve mitochondrial function of hepatic tissue in gouty mice by increasing the level of tetra 18:2 CL.

It should be noted that mitochondrial dysfunction would usually result in accumulation of ROS, leading to increased oxidative stress as well as lipid peroxidation. 4-Hydroxyalkenal species, such as HNE, are the products of lipid peroxidation of polyunsaturated FAs.[31] Their levels could serve as a key index of lipid peroxidation, reflecting the degree of oxidative stress. Thus, to assess oxidative stress, the MDMS-SL technology was performed to determine the levels of hydroxyalkenal species in hepatic tissues of mice from different groups. Intriguingly, compared with that of the control, the total amount of 4-hydroxyalkenal species in the model group significantly decreased (ie, 1.44 ± 0.06 in the control and 0.94 ± 0.09 nmol/mg protein in the model, respectively, $p < 0.05$) (Figure 5C). It was possible that high UA removed ROS due to its powerful antioxidant activity.[32] Meanwhile, with the significantly reduced level of serum UA, the total amount of 4-hydroxyalkenal

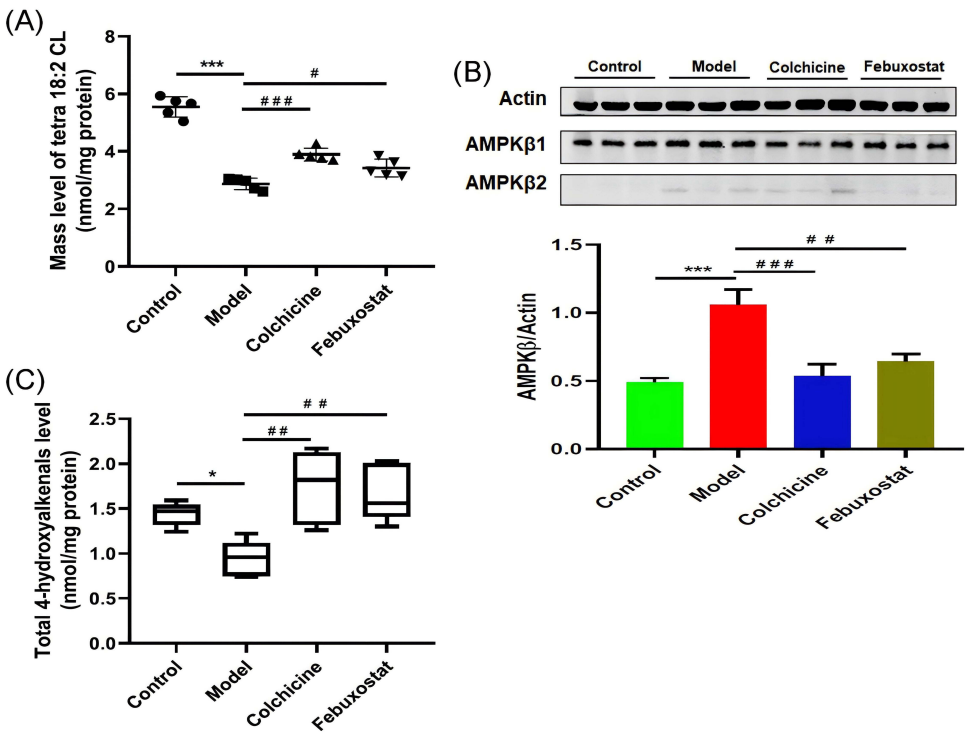

Figure 5 Lipidomics demonstrated the aberrant metabolism of mitochondrial function-related lipids in hepatic tissue of the gouty mice. Level of tetra 18:2 CL (**A**) in mouse hepatic tissue from the control, model, colchicine, and febuxostat groups (n= 5/group) were determined by the multidimensional mass-spectrometry-based shotgun lipidomics technology. Expression of AMPK protein (**B**) in hepatic tissue was measured by Western blot and expressed as fold change compared with the control. Level of 4-hydroxyalkenal species (**C**) in mouse hepatic tissue from different groups (n= 5/group) were determined by the multidimensional mass-spectrometry-based shotgun lipidomics technology. The data present means ± SEM from different groups. $^{*}p < 0.05$ and $^{***}p < 0.001$ compared with those in the control group. $^{\#}p < 0.05$, $^{\#\#}p < 0.01$, and $^{\#\#\#}p < 0.001$ compared with those in the model group. CL denotes cardiolipin.

species were markedly elevated after administration of either colchicine or febuxostat, respectively ($p < 0.01$) (Figure 5C). The result also demonstrated that ROS were eliminated by higher concentration of UA, reducing the production of 4-hydroxyalkenal species.

Alterations of Major Phospholipids and Relevant Lysophospholipids in Hepatic Tissue of Mice from Different Groups

It is well known that plasmalogens, one subclass of phospholipids, serve as endogenous antioxidant reagents, contributing to maintaining redox homeostasis.[33] Furthermore, phospholipids are also engaged in inflammation, displaying increased levels of lysophospholipids as well as lower concentrations of corresponding phospholipids.[34] Thus, the major phospholipids, including PE, PC and their corresponding lysophospholipid species (ie, LPE and LPC), in hepatic tissue of mice from different groups were also determined by using the MDMS-SL technology. It was found that the total amount of PE species decreased markedly from 67.10 ± 3.09 in the control to 55.01 ± 1.37 nmol/mg protein in the model ($p < 0.001$, Figure 6A), whereas the total level of LPE species in the model was significantly elevated ($p < 0.05$, Figure 6C). In contrast to the remarkable loss of the total content of PE species, the amount of pPE species in the model significantly increased in comparison with that of the control (4.04 ± 0.23 in the control and 5.38 ± 0.51 nmol/mg protein in the model, respectively, $p < 0.05$). Moreover, most PE species containing polyunsaturated FA (eg, 18:2, 20:4, and 22:6 FAs) markedly declined in the model group. Therefore, the result strongly suggested that inflammation instead of oxidative stress led to the alterations of PE and LPE species in hepatic tissue from the gouty mice. Incidentally, the similar alteration trends were also present in the changes of PC and LPC species in the model, although no significant differences existed between the two groups (Figure 6B and D). However, treatment with either colchicine or febuxostat had no remarkable influence on alterations of the major phospholipids and their lysophospholipids in hepatic tissue of gouty mice.

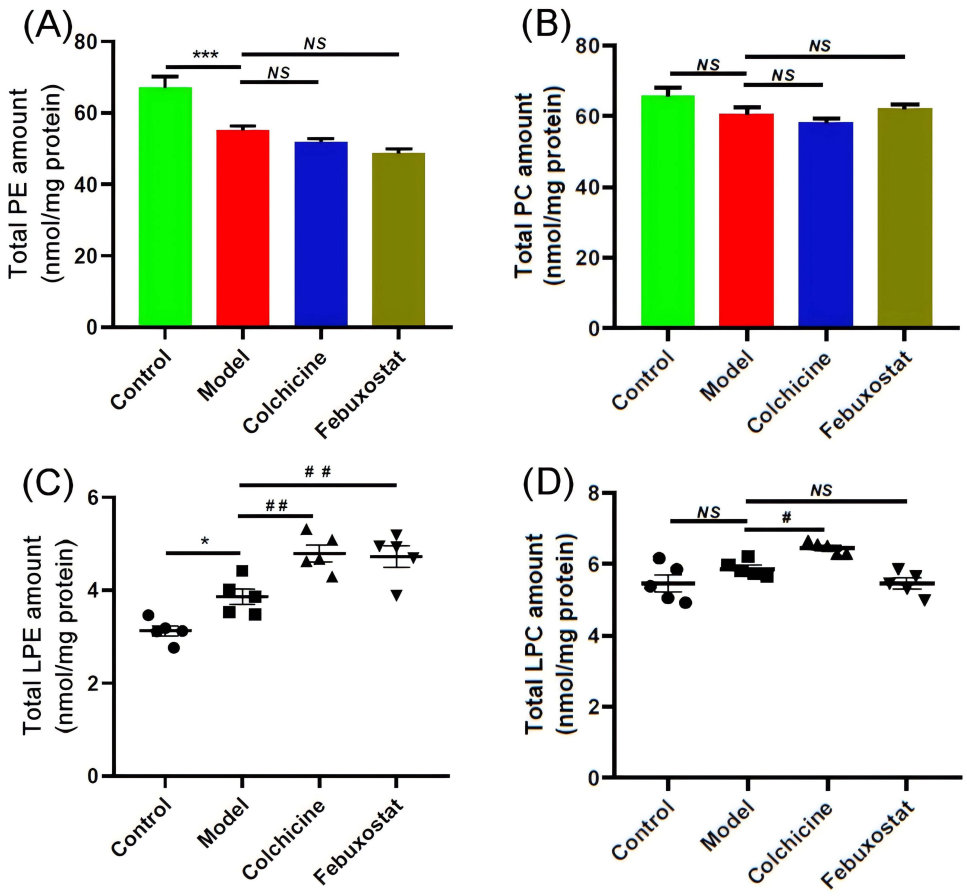

Figure 6 Alterations of major phospholipids and relevant lysophospholipids in hepatic tissue of mice from different groups. The total levels of ethanolamine glycerophospholipid (PE) **(A)**, choline glycerophospholipid (PC) **(B)**, ethanolamine lysoglycerophospholipid (LPE) **(C)**, and choline lysoglycerophospholipid (LPC) **(D)** species in mouse hepatic tissue from the control, model, colchicine, and febuxostat groups (n=5/group) were determined by the multidimensional mass-spectrometry-based shotgun lipidomics technology. The data present means ± SEM from different groups. $^{*}p < 0.05$ and $^{***}p < 0.001$ compared with those in the control group. $^{\#}p < 0.05$ and $^{\#\#}p < 0.01$ compared with those in the model group. *NS* denotes not significant.

Changes in Other Classes Phospholipids in Hepatic Tissue of Mice from Different Groups

Phospholipids are dynamically keeping homeostasis in biological systems via many interwoven pathways and networks.[8] To comprehensively reveal the aberrant metabolism of phospholipids, other important classes of phospholipids (eg, PA, PG, PS, PI, etc.) in hepatic tissue of gouty mice were also determined by the MDMS-SL technology. Figure 7 summarizes the results of lipidomics analysis for these phospholipid species. The results revealed that, compared with the controls, the levels of most individual phospholipids (ie, PG, PS, and PI) in the model were not markedly changed, except PA species (Figure 7B–D). In particular, the levels of most PA species in liver tissue of the model significantly declined in comparison with these of the control, contributing to the reduced total amount from 1537.99 ± 130.34 in the control to 980.93 ± 73.09 pmol/mg protein in the model ($p < 0.01$, Figure 7A). Furthermore, administration of either colchicine or febuxostat could significantly restore their levels in the hepatic tissue ($p < 0.05$, Figure 7A), further supporting that both of these two therapies could correct the abnormal metabolism of phospholipids to some extent.

Lipidomics Revealed Aberrant Metabolism of Sphingolipid Species in Hepatic Tissue of Mice from Different Groups

Like phospholipids, sphingolipid (eg, ceramide and SM) is an important type of lipid serving as an essential component for the plasma membrane in organisms. In the present study, the level of individual ceramide and sphingomyelin species present in liver samples of mice from different groups was also measured by the MDMS-SL technology. The lipidomics analysis demonstrated that the total amounts of ceramide (control vs model: 1.81 ± 0.07 vs 2.27 ± 0.13 nmol/mg protein, $p < 0.05$) and

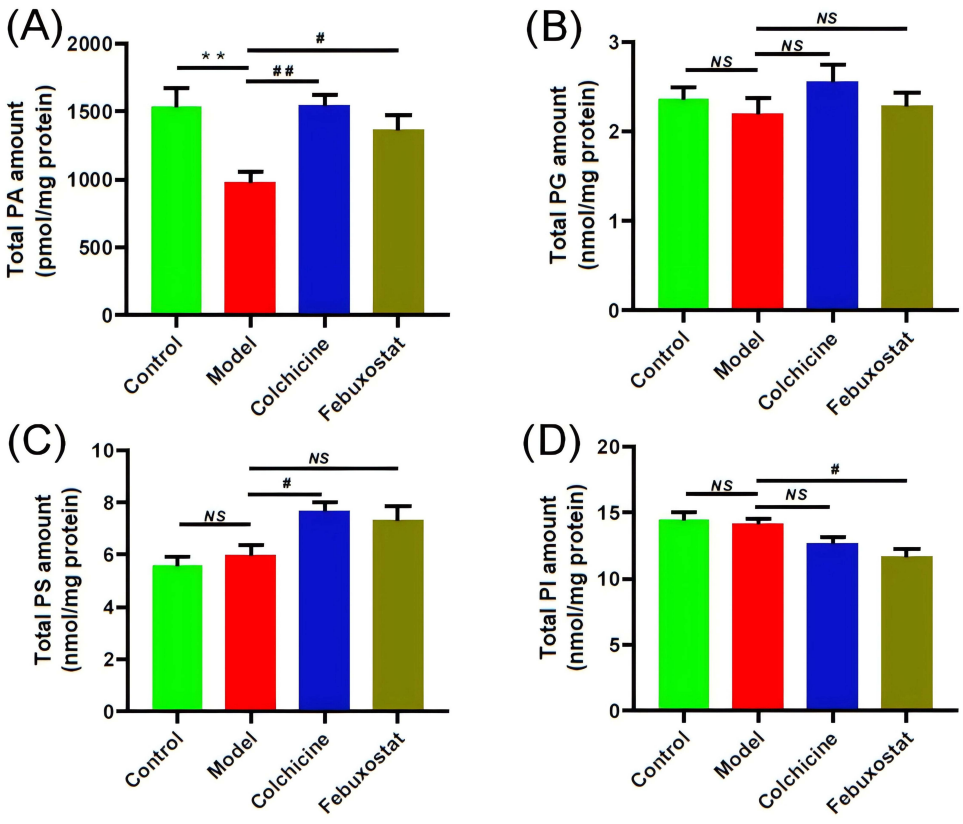

Figure 7 Changes in other classes of phospholipid species in hepatic tissue of the gouty mice. The total levels of phosphatidic acid (PA) (**A**), phosphatidylglycerol (PG) (**B**), phosphatidylserine (PS) (**C**), and phosphatidylinositol (PI) (**D**) in mouse hepatic tissue from the control, model, colchicine, and febuxostat groups (n=5/group) were determined by the multidimensional mass-spectrometry-based shotgun lipidomics technology. The data present means ± SEM from different groups. $^{**}p < 0.01$ compared with those in the control group. $^{\#}p < 0.05$ and $^{\#\#}p < 0.01$ compared with those in the model group. *NS* stands for not significant.

SM species (control vs model: 4.18 ± 0.21 vs 5.30 ± 0.33 nmol/mg protein, $p < 0.05$) in the model group showed significant increase trends compared with these of the control mice, respectively (Figure 8). Additionally, the levels of ceramide and SM species displayed declining tendency after treatment with either colchicine or febuxostat to some extent (Figure 8).

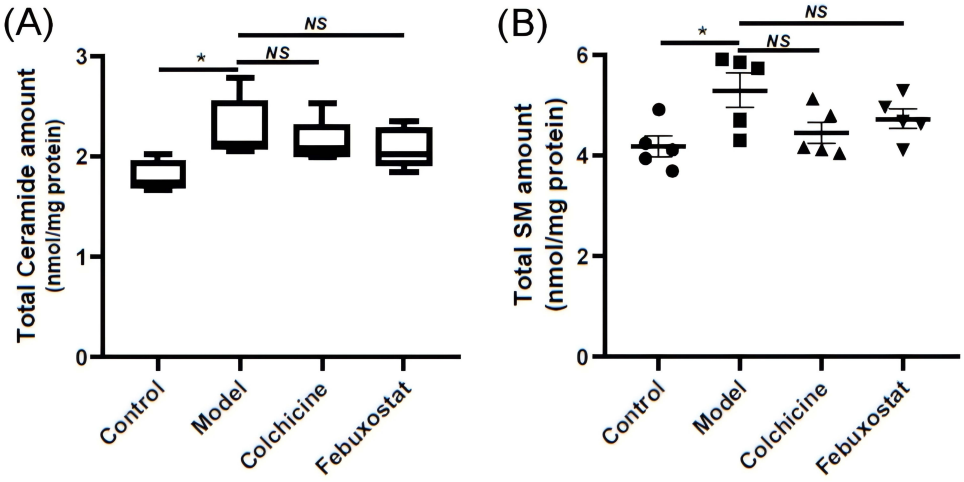

Figure 8 Lipidomics revealed aberrant metabolism of sphingolipid species in hepatic tissue of mice from different groups. The total levels of ceramide **(A)** and sphingomyelin (SM) **(B)** species in mouse hepatic tissue from the control, model, colchicine, and febuxostat groups (n= 5/group) were determined by the multidimensional mass-spectrometry-based shotgun lipidomics technology. The data present means ± SEM from different groups. $^{*}p < 0.05$ compared with those in the control group. *NS* denotes not significant.

Discussion

Accumulating evidence has shown that gout/hyperuricaemia is closely linked to the increased prevalence, incidence and severity of NAFLD, suggesting that high serum UA levels might drive NAFLD progression.[6] As aforementioned, lipids are involved in numerous biological processes, and their aberrant metabolism could contribute to the development of various major diseases, including obesity, diabetes, cancers, and autoimmune diseases.[25] In particular, the abnormal accumulation of lipids, particularly ectopic fat deposition in the liver, could significantly contribute to NAFLD development.[35] Thus, to elucidate the mechanism(s) underlying NAFLD progression and assess the effects of different therapies, the MDMS-SL technology was performed for class-targeted lipid analysis of cellular lipidomes in hepatic tissue from a gouty model with/without treatment with either colchicine or febuxostat.

In the study, the gouty model mice displayed classical characteristics of gout, including high serum UA, significant foot joint swelling, reduced footpad mechanical pain threshold, gouty inflammation including elevated levels of proinflammatory cytokines (eg, TNF-α, IL-1β, and IL-6) in serum and inflammation in the foot join, and increased XOD activity in hepatic tissue. All these indexes collectively suggested that the gouty model was well established by a combination of MSU crystal injection and HFD feeding. As anticipated, serum UA as well as other relevant indexes of gout/hyperuricaemia was significantly improved through treatment with either colchicine or febuxostat, greatly alleviating gouty symptoms of the model. Meanwhile, the reduced levels of BUN and creatinine after administration of either colchicine or febuxostat, supporting that they could also prevent renal injury in the gouty model.[13]

Lipidomics clearly revealed that not only TAG species were seriously accumulated in hepatic tissue of the gouty model but also the composition of FAs in TAG pool were significantly altered, especially 18:1 and 18:2 FAs (Figure 4). It has been widely accepted that ectopic fat deposition in hepatic tissue increases the susceptibility to risk factors for liver damage, including endoplasmic reticulum stress, perturbation of autophagy, mitochondrial dysfunction, hepatocellular apoptosis, as well as inflammatory responses.[36] Due to reduced FA β-oxidation, the triggered mitochondrial dysfunction in turn further promoted hepatic lipid droplet formation and steatosis. In addition, alteration of FA composition in TAG pool also changed melting/dropping point, crystallization behavior, thermal properties, and oxidative stability of TAG species, consequently affecting the function of liver.[13] After treatment with either colchicine or febuxostat, the ectopic fat deposition in the hepatic could be effectively relieved along with the reduced serum UA, preventing the development of NAFLD.

Lipidomics analysis also revealed that the impaired mitochondrial function was resulted by decreased tetra 18:2 CL in hepatic tissue of the gouty model, thereby leading to falling energy status. It is well known that tetra 18:2 CL is the fully functional CL species and its content reflects the mitochondrial function.[37] In addition to the fact that ectopic fat deposition in hepatic tissue could lead to mitochondrial dysfunction, decreased tetra 18:2 CL also impaired the mitochondrial function, further leading to the declined production of ATP. It has been demonstrated that mitochondrial dysfunction promotes cell death, liver fibrogenesis, inflammation, and the innate immune responses to viral infections, and these phenomena are commonly observed in liver tissue from patients with chronic liver diseases, especially NAFLD.[38] AMPK is a central cellular energy sensor, helping maintain energy homeostasis between ATP consumption and production, and it is usually simulated by energy depletion.[39] Therefore, the high expression of AMPK protein in the model group also demonstrated that ATP deficiency was present in the hepatic tissue of the gouty model (Figure 5). Meanwhile, along with the recovery of tetra 18:2 CL and the reduced serum UA in colchicine and febuxostat-treated groups, the expression of AMPK protein reduced, further suggesting that treatment with colchicine and febuxostat could relieve the ATP-deficiency status through improving mitochondrial function, and consequently prevent liver injury of the gouty model to some extent.

Additionally, the aberrant metabolism of lipids as well as higher serum UA could also cause hepatic inflammation. On the one hand, high serum UA could directly induce inflammatory responses in a crystal-dependent mechanism. For example, MSU crystals deposited in joint or the tubular interstitial space can be recognized by macrophages, resulting in chronic inflammation and tissue damage;[40] at the same time, MSU crystals could also promote secretion of chemokines (eg, CXCL-12) and proinflammatory cytokines of macrophages, such as IL-1β, IL-18, and interferons.[41] On the other hand, the aberrant lipid metabolism, particularly low HNE level, also induced inflammatory responses, promoting the progression of liver damage in the gouty model. Usually, mitochondrial dysfunction is closely associated with oxidative stress, collectively contributing to insulin resistance in patients with steatohepatitis.[42] However, in the study, lipidomics

analysis implied that oxidative stress was not increased in hepatic tissue of the gouty model for the following reasons: (1) reduced level of 4-hydroxyalkenal species (Figure 5) and (2) increased amounts of pPE and pPC species.[9] These results could be attributed to the powerful antioxidant activity of UA. Although high level of UA removed ROS, protecting the liver from damage of oxidative stress and probably inflammatory responses, it also reduced HNE bioavailability. In general, it is deemed that 4-hydroxyalkenal species are a class of toxic end products of lipid peroxidation. However, numerous studies have also indicated whether HNE species have a beneficial effect on cells/tissues or not based on their concentrations.[43] Reduced HNE bioavailability could promote expression of transcription factors Nrf2 and NF-κB, leading to the release of proinflammatory cytokines, such as TNF-α, IL-1β, and IL-8. Following this line of reasoning, administration of either colchicine or febuxostat could inhibit hepatic inflammation to prevent liver damage by both decreasing high serum UA and restoring HNE bioavailability.

In addition, the up regulation of sphingolipids in hepatic tissue also proved that hepatic damage was present in the gouty mice. Sphingolipids, in particular ceramide and SM, are among the most important biomolecules, serving as both constructive components and signal carriers in physiological processes. Accumulated studies demonstrated that elevated hepatic sphingolipid levels are present in NAFLD, and both hepatocellular lipid accumulation and chronic inflammation could drive sphingolipid production.[44,45] Therefore, the increased total amounts of both ceramide and SM species in liver sample from the gouty model were within expected and also reflected the progress of hepatic damage (Figure 8). After treatment with either colchicine or febuxostat, both of their concentrations displayed downward tendency, further demonstrating degrees of ectopic fat deposition and hepatic inflammation were ameliorated to some extent.

The strength of this study is that MDMS-SL technology was used for comprehensive and detailed lipidomic analysis of hepatic tissue. It enabled us to reveal the molecular mechanisms underlying the disease model. Additionally, by investigating the effects of colchicine and febuxostat on lipid metabolism and disease biomarkers, the study provided valuable insights into the influence of these treatments on liver function and inflammation in the gouty model. However, the conclusions of this study were only drawn from the results of the model mouse, and the underlying mechanism(s) was not further verified in related cell experiments in vitro.

Conclusions

The present study clearly demonstrated that aberrant metabolism of lipids was present in hepatic tissue of the gouty model induced by a combination of MSU crystal injection and HFD feeding. These alterations mainly included ectopic fat deposition as well as altered composition of FAs in TAG pool, impaired mitochondrial function resulted by decreased tetra 18:2 CL, and reduced HNE bioavailability led by high serum UA. In addition to inflammatory responses resulted by deposition of MSU crystals, these changes could further trigger histopathological alteration of hepatic tissue, cellular energy depletion, and hepatic inflammation, greatly contributing to the progress of liver damage to the gouty model. Administration of either colchicine or febuxostat could not only significantly relieve the gouty symptoms but also correct the aberrant metabolism of hepatic lipids, preventing liver damage in the gouty model.

Abbreviations

ADA, adenosine deaminase; AMPK, AMP-activated protein kinase; BUN, blood urea nitrogen; CL, cardiolipin; FA, fatty acyl; H&E, hematoxylin and eosin; HFD, high-fat diet; HNE, 4-hydroxy-2(*E*)-nonenal; MDMS-SL, multi-dimensional mass spectrometry-based shotgun lipidomics; MSU, monosodium urate; NAFLD, non-alcoholic fatty liver disease; PA, phosphatidic acid; PC, choline glycerophospholipid; LPC, choline lysoglycerophospholipid; PE, ethanolamine glycerophospholipid; LPE, ethanolamine lysoglycerophospholipid; PG, phosphatidylglycerol; PI, phosphatidylinositol; PS, phosphatidylserine; ROS, reactive oxygen species; SM, sphingomyelin; TAG, triglyceride; UA, uric acid; XOD, xanthine oxidase.

Data Sharing Statement

The data that support the findings of this are available from the corresponding author, C.H., upon reasonable request.

Author Contributions

All authors made a significant contribution to the work reported, whether that is in the conception, study design, execution, acquisition of data, analysis and interpretation, or in all these areas; took part in drafting, revising or critically reviewing the article; gave final approval of the version to be published; have agreed on the journal to which the article has been submitted; and agree to be accountable for all aspects of the work.

Ethics Approval

The animal study protocol was approved by the Ethics Committee of Zhejiang Chinese Medical University with approved No. IACUC-20220913-16 at 13 Sep 2022.

Funding

The work was partially supported by the National Natural Science Foundation of China (No. 82274230), Natural Science Foundation of Zhejiang Province of China (No. LQ23H290002), and Research Project of Zhejiang Chinese Medical University (No. 2024JKZKTS02).

Disclosure

The authors declare that there are no conflicts of interest.

References

1. Dalbeth N, Gosling AL, Gaffo A, Abhishek A. Gout. *Lancet*. 2021;397(10287):1843–1855. doi:10.1016/S0140-6736(21)00569-9
2. Richette P, Doherty M, Pascual E, et al. 2018 updated European league against rheumatism evidence-based recommendations for the diagnosis of gout. *Ann Rheum Dis*. 2020;79(1):31–38. doi:10.1136/annrheumdis-2019-215315
3. Dalbeth N, Merriman TR, Stamp LK. Gout. *Lancet*. 2016;388(10055):2039–2052. doi:10.1016/S0140-6736(16)00346-9
4. Desai J, Steiger S, Anders HJ. Molecular pathophysiology of gout. *Trends Mol Med*. 2017;23(8):756–768. doi:10.1016/j.molmed.2017.06.005
5. Kuo CF, Yu KH, Luo SF, et al. Gout and risk of non-alcoholic fatty liver disease. *Scand J Rheumatol*. 2010;39(6):466–471. doi:10.3109/03009741003742797
6. Xu C. Hyperuricemia and nonalcoholic fatty liver disease: from bedside to bench and back. *Hepatology International. Mar.* 2016;10(2):286–293. doi:10.1007/s12072-015-9682-5
7. Sun Q, Zhang T, Manji L, et al. Association between serum uric acid and non-alcoholic fatty liver disease: an updated systematic review and meta-analysis. *Clin Epidemiol*. 2023;15:683–693. doi:10.2147/clep.s403314
8. Han X. Lipidomics for studying metabolism. *Nat Rev Endocrinol*. 2016;12(11):668–679. doi:10.1038/nrendo.2016.98
9. Hu C, Zhang J, Hong S, et al. Oxidative stress-induced aberrant lipid metabolism is an important causal factor for dysfunction of immunocytes from patients with systemic lupus erythematosus. *Free Radic Biol Med*. 2021;163:210–219. doi:10.1016/j.freeradbiomed.2020.12.006
10. Zhang J, Lu L, Tian X, et al. Lipidomics revealed aberrant lipid metabolism caused by inflammation in cardiac tissue in the early stage of systemic lupus erythematosus in a murine model. *Metabolites*. 2022;12(5):415. doi:10.3390/metabo12050415
11. Abbott CE, Xu R, Sigal SH. Colchicine-induced hepatotoxicity. *ACG Case Rep J*. 2017;4(1):e120. doi:10.14309/crj.2017.120
12. Paschos P, Athyros VG, Tsimperidis A, Katsoula A, Grammatikos N, Giouleme O. Can serum uric acid lowering therapy contribute to the prevention or treatment of nonalcoholic fatty liver disease? *Curr Vasc Pharmacol*. 2018;16(3):269–275. doi:10.2174/1570161115666170621082237
13. Hao G, Xu X, Song J, Zhang J, Xu K. Lipidomics analysis facilitate insight into the molecular mechanisms of urate nephropathy in a gout model induced by combination of MSU crystals injection and high-fat diet feeding. *Front Mol Biosci*. 2023;10:1190683. doi:10.3389/fmolb.2023.1190683
14. Lin X, Shao T, Huang L, et al. Simiao decoction alleviates gouty arthritis by modulating proinflammatory cytokines and the gut ecosystem. *Front Pharmacol*. 2020;11:955. doi:10.3389/fphar.2020.00955
15. Wen X, Lou Y, Song S, et al. Qu-Zhuo-Tong-Bi decoction alleviates gouty arthritis by regulating butyrate-producing bacteria in mice. *Front Pharmacol*. 2020;11:610556. doi:10.3389/fphar.2020.610556
16. Lin X, Shao T, Wen X, Wang M, Wen C, He Z. Combined effects of MSU crystals injection and high fat-diet feeding on the establishment of a gout model in C57BL/6 mice. *Adv Rheumatol*. 2020;60(1):52. doi:10.1186/s42358-020-00155-3
17. Chaplan SR, Bach FW, Pogrel JW, Chung JM, Yaksh TL. Quantitative assessment of tactile allodynia in the rat paw. *J Neurosci Methods*. 1994;53(1):55–63. doi:10.1016/0165-0270(94)90144-9
18. Hu C, Du Y, Xu X, et al. Lipidomics revealed aberrant metabolism of lipids including FAHFAs in renal tissue in the progression of lupus nephritis in a murine model. *Metabolites*. 2021;11(3):142. doi:10.3390/metabo11030142
19. Hu C, Wang Y, Fan Y, et al. Lipidomics revealed idiopathic pulmonary fibrosis-induced hepatic lipid disorders corrected with treatment of baicalin in a murine model. *AAPS J*. 2015;17(3):711–722. doi:10.1208/s12248-014-9714-4
20. Bligh EG, Dyer WJ. A rapid method of total lipid extraction and purification. *Canadian Journal of Biochemistry and Physiology*. 1959;37(1):911–917. doi:10.1139/o59-099
21. Han X, Yang K, Cheng H, Fikes KN, Gross RW. Shotgun lipidomics of phosphoethanolamine-containing lipids in biological samples after one-step in situ derivatization. *J Lipid Res*. 2005;46(7):1548–1560. doi:10.1194/jlr.D500007-JLR200
22. Wang M, Fang H, Han X. Shotgun lipidomics analysis of 4-hydroxyalkenal species directly from lipid extracts after one-step in situ derivatization. *Anal Chem*. 2012;84(10):4580–4586. doi:10.1021/ac300695p

23. Sun C, Ma C, Li L, Han Y, Wang D, Wan X. A novel on-tissue cycloaddition reagent for mass spectrometry imaging of lipid C=C position isomers in biological tissues. *Chin Chem Lett*. 2022;33(4):2073–2076. doi:10.1016/j.cclet.2021.08.034
24. Yang K, Cheng H, Gross RW, Han X. Automated lipid identification and quantification by multidimensional mass spectrometry-based shotgun lipidomics. *Anal Chem*. 2009;81(11):4356–4368. doi:10.1021/ac900241u
25. Hu C, Luo W, Xu J, Han X. Recognition and avoidance of ion source-generated artifacts in lipidomics analysis. *Mass Spectrom Rev*. 2022;41(1):15–31. doi:10.1002/mas.21659
26. Han X, Gross RW. Shotgun lipidomics: electrospray ionization mass spectrometric analysis and quantitation of cellular lipidomes directly from crude extracts of biological samples. *Mass Spectrom Rev*. 2005;24(3):367–412. doi:10.1002/mas.20023
27. So AK, Martinon F. Inflammation in gout: mechanisms and therapeutic targets. *Nat Rev Rheumatol*. 2017;13(11):639–647. doi:10.1038/nrrheum.2017.155
28. Lanaspa MA, Sanchez-Lozada LG, Choi Y-J, et al. Uric acid induces hepatic steatosis by generation of mitochondrial oxidative stress. *J Biol Chem*. 2012;287(48):40732–40744. doi:10.1074/jbc.M112.399899
29. He Q, Han X. Cardiolipin remodeling in diabetic heart. *Chem Phys Lipids*. 2014;179:75–81. doi:10.1016/j.chemphyslip.2013.10.007
30. Herzig S, Shaw RJ. AMPK: guardian of metabolism and mitochondrial homeostasis. *Nat Rev Mol Cell Biol*. 2018;19(2):121–135. doi:10.1038/nrm.2017.95
31. Hu C, Wang M, Han X. Shotgun lipidomics in substantiating lipid peroxidation in redox biology: methods and applications. *Redox Biol*. 2017;12:946–955. doi:10.1016/j.redox.2017.04.030
32. El Ridi R, Tallima H. Physiological functions and pathogenic potential of uric acid: a review. *J Adv Res*. 2017;8(5):487–493. doi:10.1016/j.jare.2017.03.003
33. Hu C, Zhou J, Yang S, et al. Oxidative stress leads to reduction of plasmalogen serving as a novel biomarker for systemic lupus erythematosus. *Free Radic Biol Med*. 2016;101:475–481. doi:10.1016/j.freeradbiomed.2016.11.006
34. Knuplez E, Marsche G. An updated review of pro- and anti-Inflammatory properties of plasma lysophosphatidylcholines in the vascular system. *Int J Mol Sci*. 2020;21(12):4501. doi:10.3390/ijms21124501
35. Younossi Z, Koenig A, Abdelatif D, Fazel Y, Henry L, Wymer M. Global epidemiology of nonalcoholic fatty liver disease-meta-analytic assessment of prevalence, incidence, and outcomes. *Hepatology*. 2016;64(1):73–84. doi:10.1002/hep.28431/suppinfo
36. Lian CY, Zhai ZZ, Li ZF, Wang L. High fat diet-triggered non-alcoholic fatty liver disease: a review of proposed mechanisms. *Chem Biol Interact*. 2020;330:109199. doi:10.1016/j.cbi.2020.109199
37. Sparagna GC, Chicco AJ, Murphy RC, et al. Loss of cardiac tetralinoleoyl cardiolipin in human and experimental heart failure. *J Lipid Res*. 2007;48(7):1559–1570. doi:10.1194/jlr.M600551-JLR200
38. Mansouri A, Gattolliat CH, Asselah T. Mitochondrial dysfunction and signaling in chronic liver diseases. *Gastroenterology*. 2018;155(3):629–647. doi:10.1053/j.gastro.2018.06.083
39. Lin SC, Hardie DG. AMPK: sensing glucose as well as cellular energy status. *Cell Metab*. 2018;27(2):299–313. doi:10.1016/j.cmet.2017.10.009
40. Su HY, Yang C, Liang D, Liu HF. Research advances in the mechanisms of hyperuricemia-induced renal injury. *Biomed Res Int*. 2020;2020:5817348. doi:10.1155/2020/5817348
41. Välimäki E, Miettinen JJ, Lietzén N, Matikainen S, Nyman TA. Monosodium urate activates Src/Pyk2/PI3 kinase and cathepsin dependent unconventional protein secretion from human primary macrophages. *Mol Cell Proteomics*. 2013;12(3):749–763. doi:10.1074/mcp.M112.024661
42. Koliaki C, Szendroedi J, Kaul K, et al. Adaptation of hepatic mitochondrial function in humans with non-alcoholic fatty liver is lost in steatohepatitis. *Cell Metab*. 2015;21(5):739–746. doi:10.1016/j.cmet.2015.04.004
43. Sharma S, Sharma P, Bailey T, et al. Electrophilic aldehyde 4-hydroxy-2-nonenal mediated signaling and mitochondrial dysfunction. *Biomolecules*. 2022;12(11):1555. doi:10.3390/biom12111555
44. Day CP, Saksena S. Non-alcoholic steatohepatitis: definitions and pathogenesis. *J Gastroenterol Hepatol*. 2002;Suppl 3:S377–84. doi:10.1046/j.1440-1746.17.s3.31.x
45. Bikman BT, Summers SA. Sphingolipids and hepatic steatosis. *Adv Exp Med Biol*. 2011;721:87–97. doi:10.1007/978-1-4614-0650-1_6